J. Coat. Technol. Res., **16** (5) 1493–1502, 2019
https://doi.org/10.1007/s11998-019-00224-3

Phosphorus-containing reactive agent for UV-curable flame-retardant wood coating

Saket Mulge, Siddhesh Mestry, Durva Naik, Shashank Mhaske

Abstract An attempt to develop a phosphorus-based flame-retardant UV-curable agent (UV-RA) for coating application led to the synthesis of a reactive compound which can be used as crosslinker along with UV-curable epoxy acrylate oligomer to form a coating. UV-RA was characterized via FTIR, NMR, hydroxyl, and iodine values. Study based on the effects of varying amount of UV-RA incorporated in the formulation was investigated by checking thermal, mechanical, and flame-retardant properties. An enhancement in all the properties was observed with an increase in concentration of UV-RA and each coating containing UV-RA successfully portrayed flame-retardant properties. The highest loss on ignition (LOI) value obtained was 27 while the initial and final degradation temperatures increased along with the char yield. The mechanical properties did not vary much except for the low values for 20UV-RA.

Keywords UV-curable coating, crosslinking agent, flame-retardant, phenylphosphonic dichloride

Introduction

Wood, a lightweight and flexible material composed of cellulose, hemicellulose, and lignin is widely used for construction applications. It is strong, stiff, and sustainable due to its natural availability.[1,2] However, it is highly susceptible to fire. Therefore, flame-retardant (FR) wood coatings are employed which retard ignition and rate of spread of flames.[3,4]

Traditional nonintumescent flame-retardant coatings are either made of halogen-based compounds or by incorporating inorganic metal compounds in the formulation.[5,6] These compounds prevent the spread of flame either via radical quenching or by the formation of glassy protective layers rather than forming blown voluminous char during combustion.[7–9] Owing to the lower number of flame-retardant components in nonintumescent coating systems, they are more compatible with the polymeric matrices leading to better mechanical and fire performance properties. Though halogenated FR systems are effective and popular, they have plenty of drawbacks due to their harmful nature as they work in the gas phase by acting as free radical scavengers and hence are not eco-friendly. Thus, they have come under scrutiny in recent years and researchers have started to look for possible efficient alternatives which mainly include nonintumescent-type flame retardants based on chemical compounds containing phosphorus, nitrogen, silicon, etc.[10] In the case of phosphorous-based flame retardants, they produce less smoke and toxic gases during combustion and also demonstrate action in both gas phase and condensed phase.[11,12] Phosphorous can also be incorporated either as an additive or by reacting and making it a part of the polymer chain. Nevertheless, phosphorous additives usually suffer from poor compatibility with the base polymer and tend to leach out. They are required in high amounts which affect the processability and mechanical properties. For instance, a higher amount of incorporation results in a greater number of volatiles produced, thus increasing the final cost of the product. On the other hand, reactive type of flame retardants offers various advantages such as better flame retardancy, superior adhesion, improved dye-

S. Mulge, S. Mestry, D. Naik, S. Mhaske (✉)
Department of Polymer and Surface Engineering, Institute of Chemical Technology, Mumbai, India
e-mail: stmhaske@gmail.com

S. Mulge
e-mail: iamsam9617@gmail.com

S. Mestry
e-mail: siddhesh17mestry@gmail.com

D. Naik
e-mail: durvanaikict@gmail.com

ability, higher antistatic properties, and enhanced solubility to the polymer.[12] P-N-based synergism is one such highly studied system. In such systems, phosphorus component is reduced, which in turn reduces the cost of the formulation, while simultaneously preserving or even improving the coating performance like flame retardancy, mechanical, physical, and chemical properties, etc. Furthermore, it is even possible to introduce tailored functionalities like a crosslinking agent or a reactive diluent.[13] Furthermore, ultraviolet (UV)-light curing techniques are being increasingly used in industrial flame-retardant coating applications due to their advantageous characteristics such as rapid curing, low energy consumption, and reduced environmental pollution.[13–15] These coatings exhibit high chemical stability with low volatile organic compounds (VOC) emission.

In this work, phosphorus-containing reactive agent was synthesized using phenyl phosphonic dichloride, ethanolamine, and glycidyl methacrylate. This agent was used as a reactive component in UV-curable epoxy acrylate oligomer to impart flame-retardant property. The concentration of the synthesized component was varied to observe the effect on flame retardancy and several other coating properties after photopolymerization.

Materials and methods

Materials

Ethanolamine, hydroquinone (HQ), sodium hydroxide (NaOH) pellets, hydroquinone (HQ), tetramethylolpropyl triacrylate (TMPTA), ethyl acetate (EA), and acetone were purchased from S D Fine-Chem. Ltd, India.. Epoxy acrylate oligomer (DESMOLUX- 2266) was provided by Bayer Materials, India. Photoinitiator (Irgacure 184) was received from BASF Pvt. Ltd., India. Glycidyl methacrylate (GMA) and phenylphosphonic dichloride (PPDC) were procured from Alfa Aesar, India and Sigma-Aldrich, India, respectively. Triethylamine (TEA) was obtained from Rankem Chemicals, India. All the chemicals were of laboratory grade and used as procured without any treatment.

Reaction of ethanolamine and PPDC

In a four-necked round-bottom flask equipped with a mechanical stirrer, a condenser and a nitrogen balloon, ethanolamine (11.75 g, 0.19 mol), and TEA (19.48 g, 0.19 mol) were added along with 40 mL acetone. PPDC (18.76 g, 0.96 mol) was added dropwise maintaining the temperature between 0°C and 5°C using the ice bath. The reaction was continuously stirred at room temperature for 24 h, and EA and deionized water were added to separate the organic and aqueous phases. The organic solvent was then recovered under vacuum to get the desired intermediate (I-1) (yield = 83.71%). The reaction scheme for the synthesis of I-1 is shown in Fig. 1. (*CHNS analysis: C* = 49.18, H* = 7.02, N* = 11.47, C = 48.73, H = 8.48, N = 11.09, *theoretical*).

Reaction of I-1 with GMA

In a three-necked round-bottom flask equipped with mechanical stirrer and a condenser, GMA (5 g, 0.035 mol) was added along with HQ (0.5 wt% of the total batch) and stirred for 2 h at 60°C in 20 mL acetone. I-1 (4.29 g, 0.017 mol) and NaOH (0.7 g, 0.017 mol) were added in the reaction mixture followed by stirring at 100°C for 5 h. Then, the layer separation was instigated using EA and water. EA was recovered under vacuum to get the reactive agent for UV-curable coating system (UV-RA) (yield = 82.7%). The reaction scheme for the synthesis of UV-RA is shown in Fig. 2. (*CHNS analysis: C* = 50.85, H* = 6.19, N* = 5.93, C = 50.12, H = 8.03, N = 5.21, *theoretical*).

Preparation of UV-curable wood coatings

UV-curable formulations were prepared by mixing epoxy acrylate oligomer and UV-RA in various weight fractions (0–40%), with constant amount of photoinitiator (3 wt%) and TMPTA as a reactive diluent (15%). The prepared formulations were coated onto prepared wood panels (7.5 cm × 7 cm) using a brush applicator, obtaining a uniform layer. Free films were prepared by pouring the liquid formulations onto a Teflon mold. Finally, the wet formulations were hardened by exposing the coated substrates to UV irradiation by medium-pressure mercury lamp (365 nm) built into a UV curer. The speed of the belt was kept at 25 m/min with the exposure time of 20 s. The detailed formulations for the UV-curable wood coatings are tabulated in Table 1.

Characterization

ASTM D1957-86 and ASTM D1959-97 were used to determine the hydroxyl and the iodine value, respectively.

To determine the gel content, the cured films were carefully peeled off from the Teflon sheet. The known weight of polymer film was kept in the solvent mixture (50:50) of xylene and dimethyl formamide (DMF) at room temperature for 24 h followed by drying of the film at 80°C until constant weight was achieved. The gel content of the cured film was then determined by the formula:

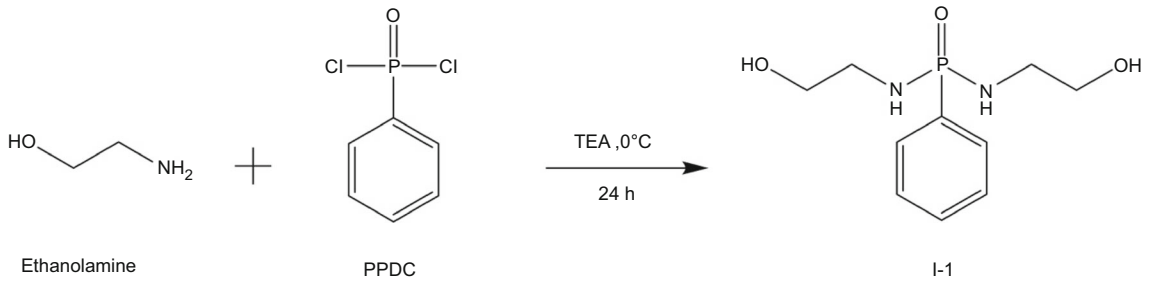

Fig. 1: Reaction scheme for the synthesis of I-1

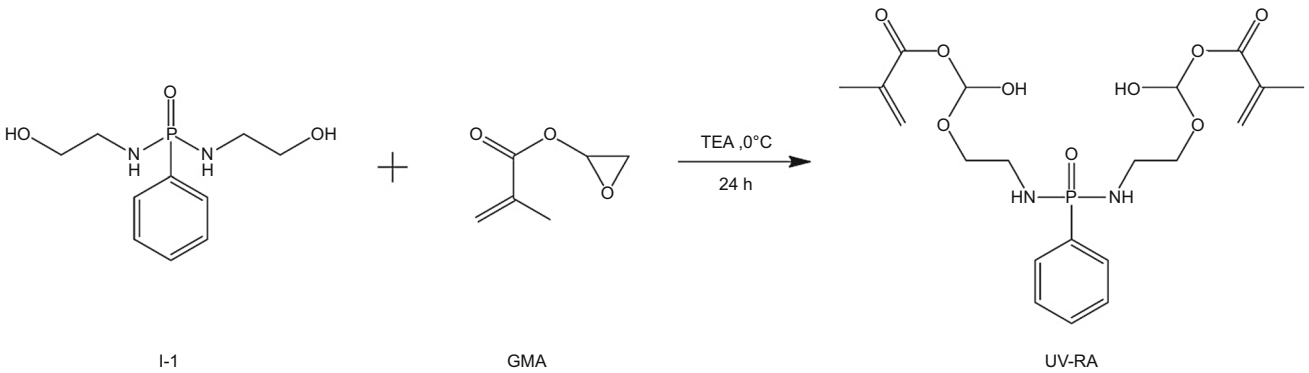

Fig. 2: Reaction scheme for the synthesis of UV-RA

Table 1: Formulations of UV-curable coatings

	FR0	FR5	FR10	FR15	FR20
Oligomer	82	77	72	67	62
TMPTA	15	15	15	15	15
Photoinitiator	3	3	3	3	3
UV-RA	0	5	10	15	20

$$\text{Gel content}(\%) = \frac{\text{Initial weight of the coating}}{\text{Weight of the coating after 24 h of solvent immersion}} \times 100$$

ASTM D570 was used to determine the water absorption of the cured coating film in which the film was weighed before soaking into the water for 24 h. After 24 h, the film was removed from the water and dried with a paper towel to achieve a constant weight. Water absorption was determined from the differences in the weight of samples before and after soaking the water according to the following equation:

$$\text{Water absorption}(\%) = \frac{(Wf - Wi)}{Wi} \times 100$$

where Wf = final weight of the coating after water absorption test and Wi = initial weight of the coating before water absorption test.

Adhesion of the coating film to the substrate was estimated according to ASTM D3359. Lattice marking of 1 cm^2 was done on the coating surface until the metal surface was exposed followed by the application of adhesion tape over the lattice marking. The adhesion tape was then pulled out from the coating surface, and adhesion failure was examined over the lattice marking. ASTM D3363 was used to perform a pencil hardness test by making a scratch on the coating surface using 6B to 6H range of pencils at an angle of 45°.

According to ASTM D5402-93, the solvent scrub resistance of the coatings was carried out using methyl ethyl ketone (MEK) and xylene. A piece of white cotton was saturated with solvent and rubbed over the coating samples. Gloss test of the coated samples was carried out by using digital mini gloss meter at an angle of 60° by Rhopoint gloss meter as per ASTM D523-99.

Instrumentation

Completion of the reaction of I-1 and UV-RA was confirmed by functional group identification using Bruker FTIR–attenuated total reflection (ATR) spectrophotometer, USA. The spectra were observed

between 600 and 4000 cm^{-1}. The supportive confirmation of the chemical structure of the final product was given by ^{1}H, ^{13}C, and ^{31}P NMR spectroscopy. ^{1}H and ^{13}C NMR spectra of the product were analyzed using Bruker DPX 800 MHz spectrophotometer with dimethyl sulfoxide (DMSO) as a solvent. The CHNS elemental analysis of compounds was done using Thermo Scientific™ FLASH™ 2000 Organic Elemental Analyzer (OEA). Combustion of the samples was done at the elevated temperature of around 1100°C in the presence of excess oxygen. Produced CO_2, H_2, and NO_2 gases were mixed and homogenized in a chamber before separation by gas chromatography followed by detection with the thermal detector. The results were reported as a percent by weight of each element. TGA of cured films was conducted on PerkinElmer TGA 4000 instrument under nitrogen and air atmosphere. Thermal analysis monitored in the temperature range of 40°C–700°C with 20°C/min heating rate. The glass transition temperature (T_g) of cured films was estimated using DSC on a PerkinElmer DSC instrument. The film sample was weighed accurately in an aluminum pan and heated from 30°C to 200°C temperature range with a heating rate of 10° C/min under nitrogen. The fire-retardant capability of the cured samples was investigated by LOI test and carried out on Dynisco, USA, according to ASTM D2863 procedure. ASTM D1356-2005 was used to carry out the UL-94 vertical burning test. Sample specimens having a size of 125 × 12.5 × 3 mm were mounted vertically, and the flame was introduced for 10 s to the specimen at an angle of 45°. The VTM ratings as shown in Table 2 were used to rate the performance of the coatings in UL-94 test.

Results and discussion

The iodine value of UV-RA was estimated using Wijs method and was found to be 604.38 mg of I_2/g of the sample which is comparable to the theoretical iodine value, i.e., 657.01 mg of I_2/g of the sample. The hydroxyl value of I-1 was found to be 448.37 mg of KOH/g of the sample compared to the theoretical value of 459.57 mg of KOH/g of the sample which confirmed the formation of the desired product.

FTIR analysis

The FTIR spectra of the ethanolamine, I-1, and UV-RA are given in Fig. 3. The peaks at 3350 cm^{-1}, 3286 cm^{-1}, and 3169 cm^{-1} in the spectrum of ethanolamine correspond to -OH and -NH_2 present in the molecule while 2921 cm^{-1} and 2855 cm^{-1} show the presence of -CH_2 present in the aliphatic chain. The peak at 1597 cm^{-1} attributes to the -NH- vibrations. The peaks at 1458 cm^{-1} and 1355 cm^{-1} correspond to the -CH- deformation vibrations while the peaks at 1076 cm^{-1} and 1031 cm^{-1} show the presence of -C-O- stretching vibrations. In the FTIR spectrum of I-1, the peaks of NH_2 vibrations diminish while only the plateau region of -OH stretching vibration remains which suggests the reaction has moved in the forward direction. Also, the sharp peak at 1022 cm^{-1} corresponds to the -P-N- linkage which confirms successive formation of the desired product. FTIR spectrum of UV-RA shows the characteristic peak at 1702 cm^{-1} which corresponds to the C = O present in GMA. Also, the peaks at 1362 cm^{-1} and 1169 cm^{-1} attribute to the C = C and C-O vibrations, respectively, which confirm successful addition of the GMA in the final structure.

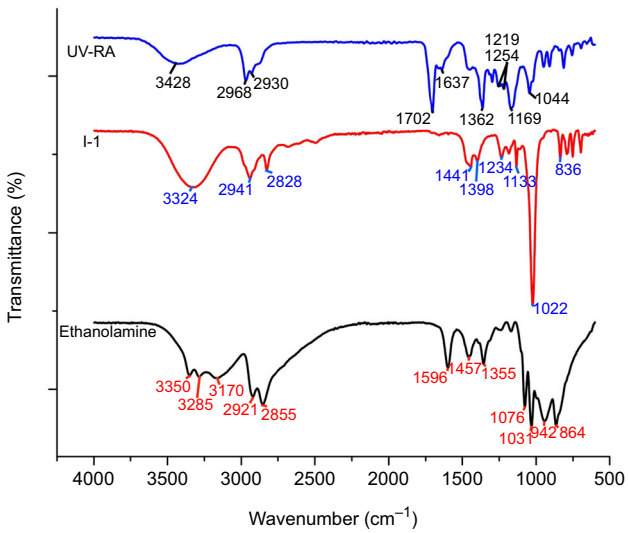

Fig. 3: FTIR spectra of ethanolamine, I-1, and UV-RA

Table 2: VTM ratings

Sr. No.	VTM rating	Description
1	VTM-0	Flame time does not exceed 10 s and inflamed dripping is not observed
2	VTM-1	Flame time ranges between 10 and 30 s but does not exceed 30 s and inflamed dripping is not observed
3	VTM-2	Flame time does not exceed 30 s and inflamed dripping is observed

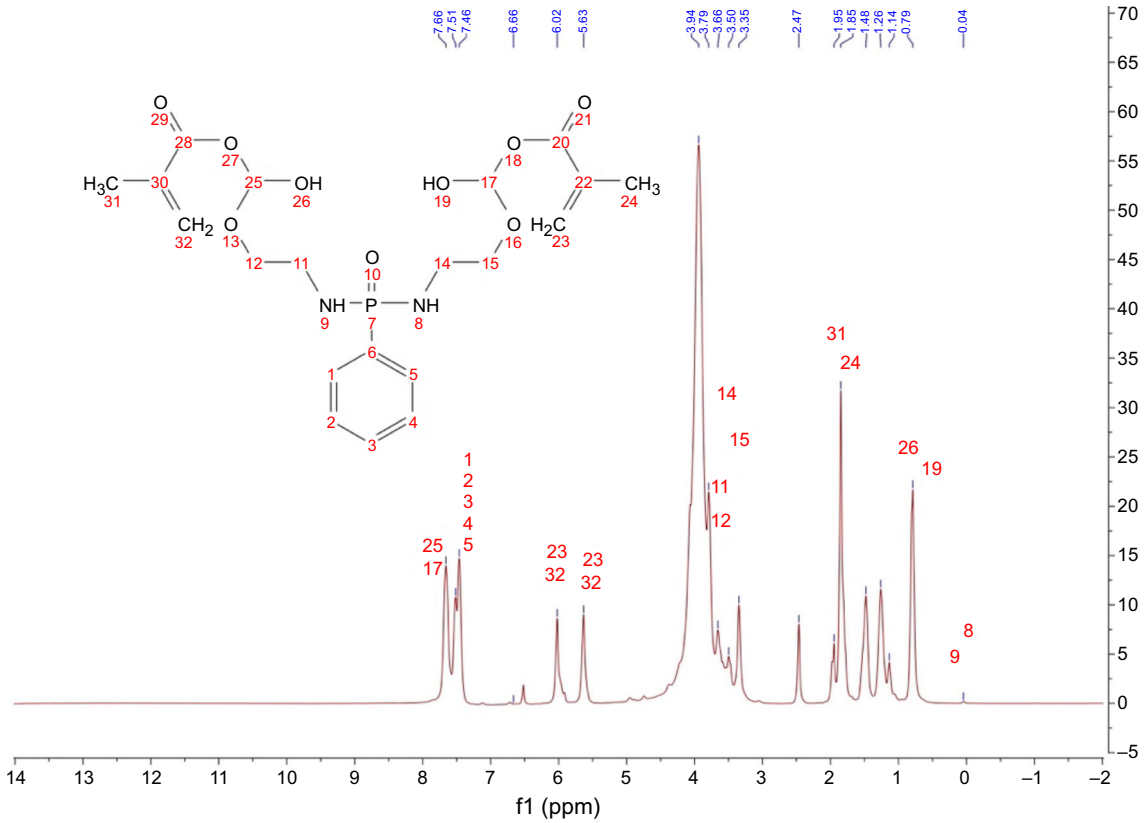

Fig. 4: ^{1}**H-NMR spectrum of UV-RA**

NMR analysis

^{1}H-NMR, ^{13}C-NMR, and ^{31}P-NMR spectra of UV-RA are shown in Figs. 4, 5, and 6, respectively. The protons of the aromatic ring are shown in the region 7.3–7.6 ppm while the aromatic carbons are between 128 and 132 ppm in the respective figures. The proton of the carbon attached to the hydroxyl group of GMA is shown at 7.66 ppm while the characteristic protons of the two hydroxyl groups of GMA are shown at 0.79 ppm. The peaks of the protons of the secondary amines are shown at 0.04 ppm. The characteristic carbons of the unsaturation present in GMA and that of CH_3 are shown at 126.07 ppm and at 18.4 ppm, respectively, in ^{13}C-NMR spectra of UV-RA. The carbons of the benzene ring are shown in the region from 128 to 132 ppm which confirms the desired structure formation. ^{31}P-NMR shows the confirmatory peak in the presence of the phosphorus in UV-RA at 26.19 ppm.

Coating properties

After application of the formulations on the wood panels, they were investigated for various properties. The properties were checked as a function of the concentration of the UV-RA and the overall structure of the coating network.

Thermal properties

Thermal properties of the formed coatings were checked using TGA and DSC. TGA graphs provide the information about the thermal degradation behavior of the coatings and allow us to predict the structural stability of the material. TGA graphs of the UV-cured films are shown in Fig. 7, and characteristic thermal degradation values are tabulated in Table 3.

The results reveal that as the phosphorus content in the backbone increases, the thermal stability of the UV-RA formulations increases. The initial degradation temperatures of all the formulations increase with the loading of phosphorus-containing moiety. The thermal stability of the coating material is dependent on the crosslinking density and the amount of thermally stable foreign moieties in the system.[16,17] Incorporation of the phosphorus-based compounds increases the thermal stability by converting themselves into phosphoric acid and water where polyphosphoric acid forms a char layer between the substrate and the flame, whereas water gives a cooling effect, thereby imparting the flame retardancy.[18,19] Owing to the bulky nature of the chemical structure of synthe-

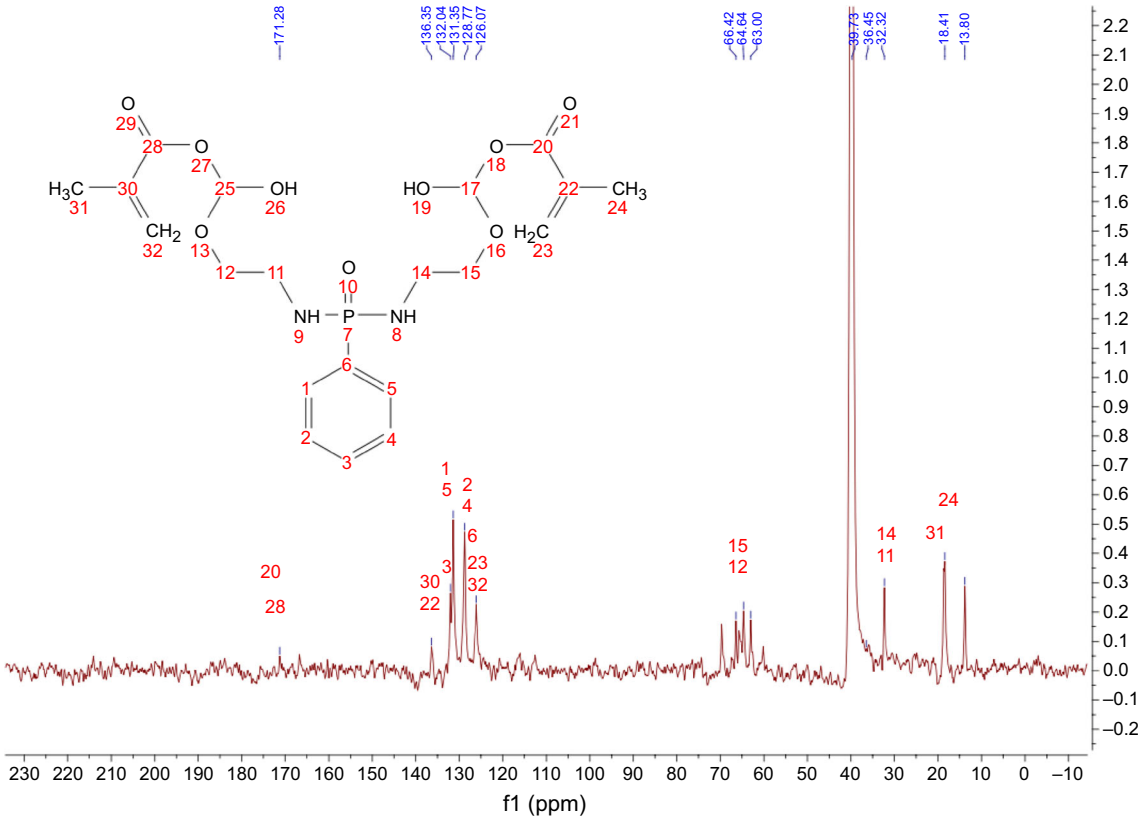

Fig. 5: ^{13}C-NMR spectrum of UV-RA

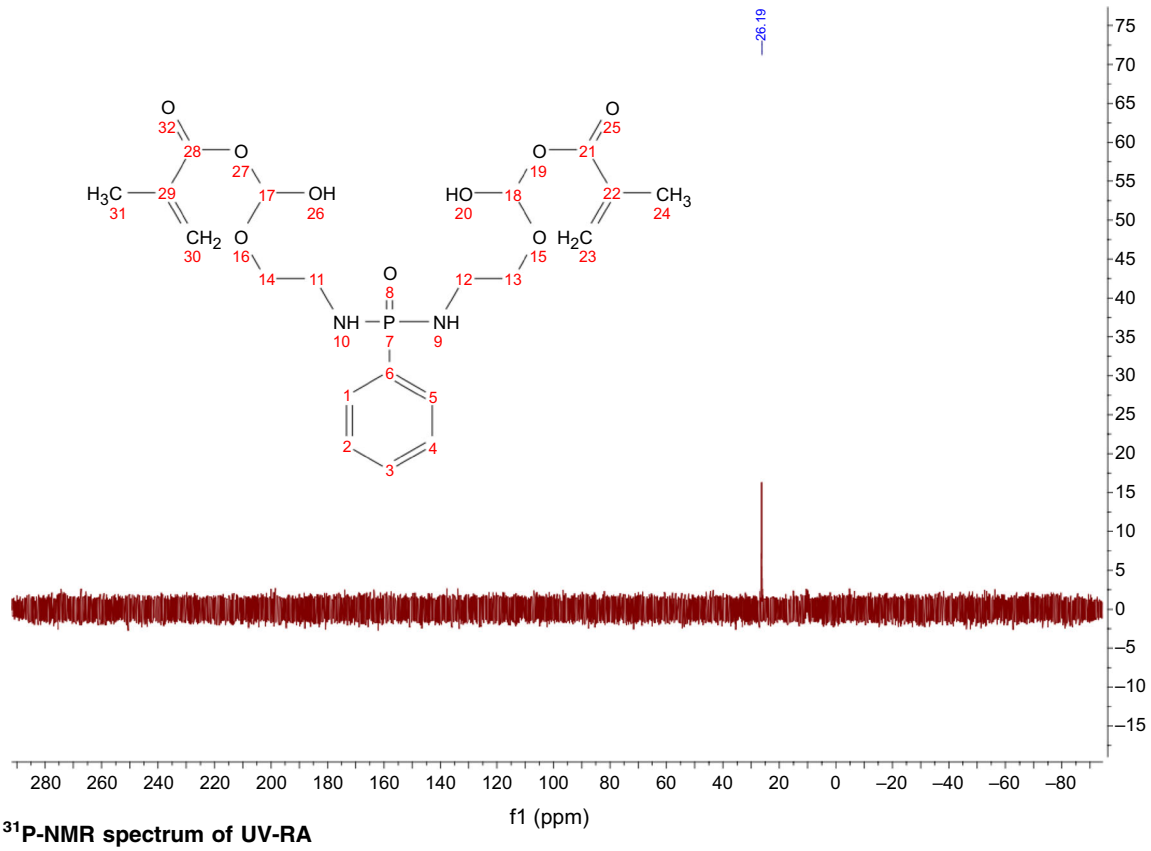

Fig. 6: ^{31}P-NMR spectrum of UV-RA

sized UV-RA, there has to be some amount of steric hindrance present for the polymer chain stacking due to the benzene ring and GMA fragments. Therefore, although the thermal stability should have increased because of increase in the phosphorus content, the effect of chemical structure of the synthesized molecule might have been reflected in the results of 15UV-RA which suggests the possibility of improper curing but increased char yield.[20,21] As seen from the results, the char yield values of the formulations increased as the loading of the UV-RA in the system increased. 40 UV-RA had the maximum amount of char yield as 14.3%. Also, the degradation characteristic values showed an increase in the initial as well as final degradation temperatures which may be attributed to the combined effect of the crosslinking density, rigidity of the benzene ring, and incorporation of the phosphorus in the system.[19,22]

The results of DSC analysis are shown in Fig. 8, and T_g values are depicted in Table 3 which determine the temperature and heat flow associated with material transitions as a function of time and temperature. The results of DSC show the increase in the T_g values as expected due to the structure of UV-RA. The phosphorus content, the benzene ring present in PPDC, and the increased crosslinking density due to multifunctional structure of UV-RA increase the brittleness and thus T_g values.[15,23] The fact of increasing voids in the system due to the bulky structure of UV-RA could have caused the coatings to have low T_g values because of improper stacking of the polymer chains. However, the rigidity of the molecule and the crosslinking density might be directing the T_g values to the higher side.

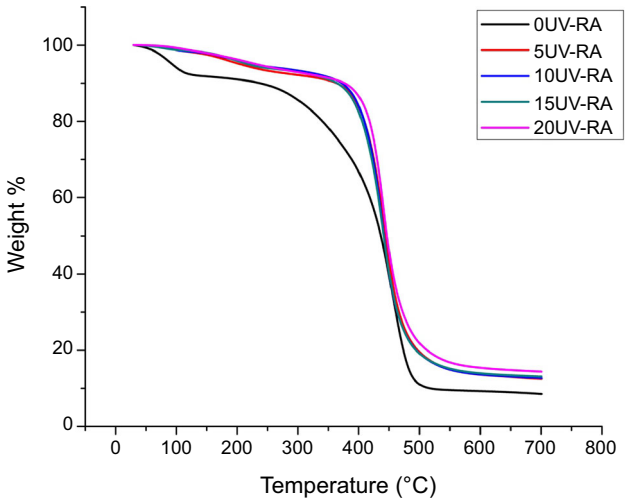

Fig. 7: TGA curves of UV-cured coatings

Mechanical properties

The mechanical properties of the coatings were checked by pencil hardness and crosshatch test. Generally, the changes in the crosslinking density obtained by the modification in the resin govern the mechanical properties, gel content, and the water absorption of the coatings.[24] Excellent mechanical properties were attributed to the strong crosslink network obtained with two-arm structure of UV-RA. As discussed in the previous sections, these results can also be related to the structure of the films. The formulations with 20% loading of UV-RA had slightly less pencil hardness rating which may be due to the increased brittleness while other films had excellent pencil hardness results. All the coatings were able to pass the crosshatch adhesion test suggesting good adhesion to the wood substrate. There was no crack observed while peeling off the tape from the substrate except for the coating with 20% loading, but there was no residue on the tape. The solvent scrub resistance is dependent partially on the adhesion of the coating to the substrate and partially on the resistance to the solvent. The prepared coatings exhibited a solvent scrub resistance with greater than 200 rubs. The gel content and water absorption are controlled by the crosslinking density and the nature of the coating. The coating showed an increase in the gel content values and a decrement in water absorption with increasing concentration of UV-RA. The obtained results are depicted in Table 4 and Fig. 9.

The flow properties, the ability to level, and the smoothness of the coating surface decide the gloss of UV-cured films. As shown in Table 4, gloss of cured coatings did not have much variation with respect to increasing concentration of UV-RA. This suggests the crosslinking might have occurred properly, and the monomers did not impede the formation of coating lattice due to steric hindrance.

Table 3: Thermal characteristic properties of UV-RA coatings

Sample	Initial degradation temperature (°C)	15% weight loss (°C)	Char yield at 700°C (%)	T_g (°C)
0UV-RA	326.1	338.5	8.0	68.4
5UV-RA	392.8	395.4	12.4	82.2
10UV-RA	393.6	396.4	12.6	92.4
15UV-RA	386.2	391.7	13.0	96.6
20UV-RA	402.1	405.6	14.3	97.3

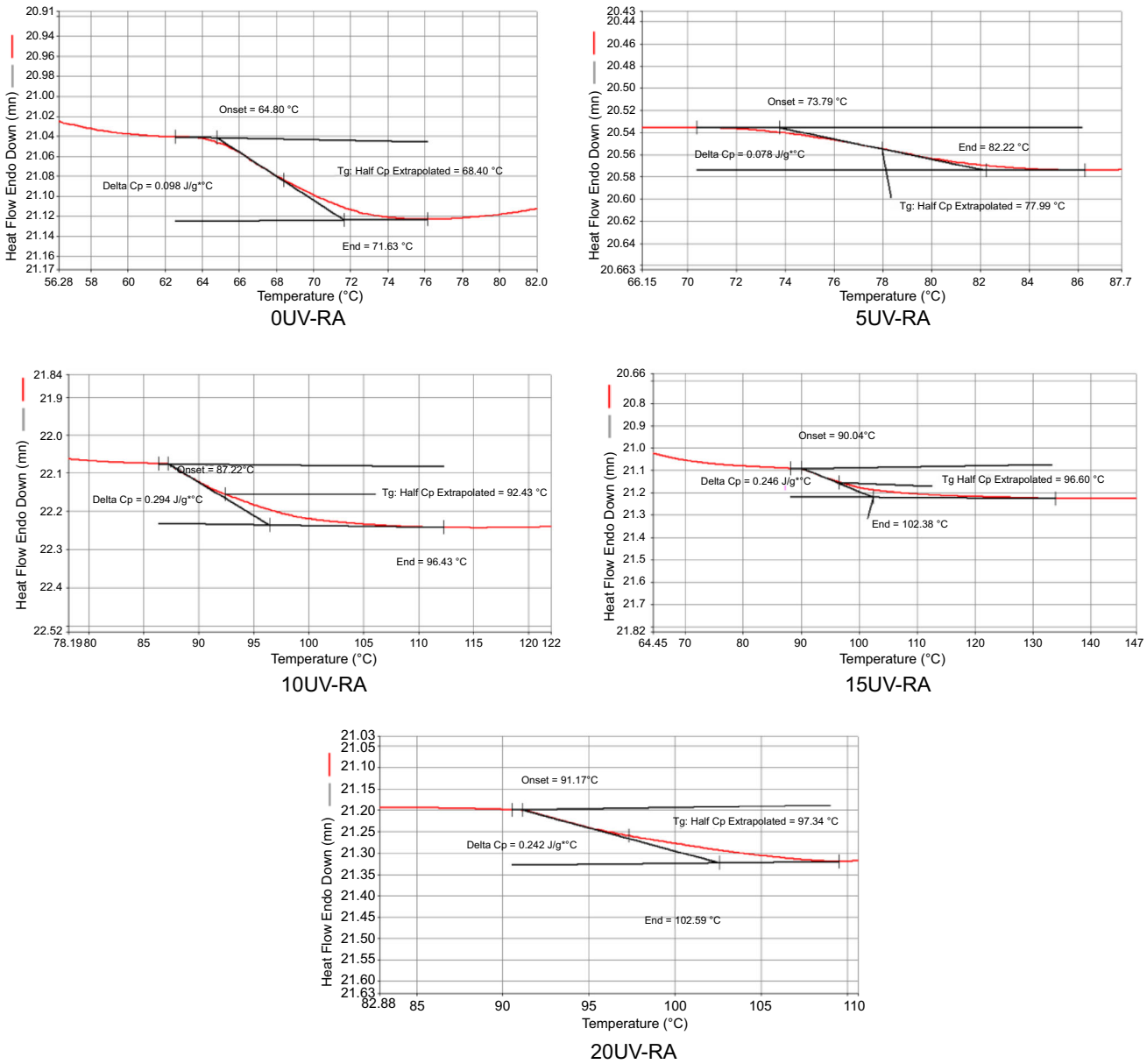

Fig. 8: DSC curves of UV-cured coatings

Table 4: Mechanical properties of UV-cured formulations

Sample	Pencil hardness	Solvent scrub test	Crosshatch test	Gloss (%)
0UV-RA, 5UV-RA	6H		Pass	125–130
10UV-RA, 15UV-RA	6H	> 200	Pass	120–125
20UV-RA	5H		Pass, observed crack on coating but no residue on adhesion tape	115–120

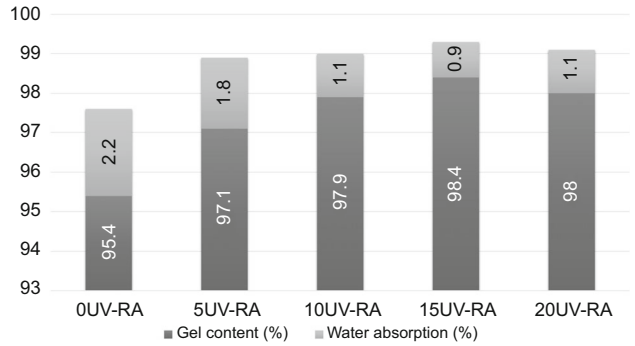

Fig. 9: Gel content and water absorption of UV-RA coatings

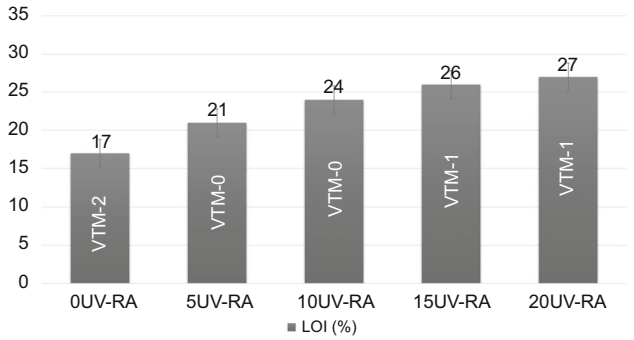

Fig. 10: LOI and VTM ratings of UV-RA coatings

Flame-retardant properties

The flame-retardant properties of the various UV-RA formulations were checked by LOI and UL-94 vertical burning tests. It was observed that the flame retardancy increased as the concentration of UV-RA in the system increased. The highest LOI was shown by 20UV-RA which can be supported by the DSC results and the char yield values of UV-RA formulations.[25–28] The crosslinking density, the phosphorus, and the rigid structure of the benzene ring played a vital role in increasing the flame retardancy of the overall system. Phosphorus has the tendency to combust at higher temperatures than polymers. The combustion of phosphorus compounds causes the formation of phosphorus-rich char layer which acts as a thermal insulator between the fire and the substrate. Hence, phosphorus compounds follow condensed phase mechanism and alter the thermal decomposition of the polymeric backbone.[29,30] The enhancement of the char layer can be done by using silicon compound along with the phosphorus compound as silicon has the capability to promote the char formation capacity of the material.[31,32]

UL-94 vertical burning test showed that 5UV-RA and 10UV-RA could self-extinguish the fire within 10 s of ignition, and the material did not drip. 15UV-RA and 20UV-RA self-extinguished the fire within 20 s of ignition with no dripping while 0UV-RA dripped during burning as there was no UV-RA present in the system. LOI values and VTM ratings of the various coating formulations are shown in Fig. 10.

Conclusion

Phosphorus-based UV-curable agent was successfully synthesized, characterized, and incorporated in various proportions into UV-curable coating. These formulations were applied to the wood panels, cured, and characterized for various thermal, mechanical, and flame-retardant properties. Thermal properties showed that the char yield values, initial degradation temperatures, and T_g values rose with the incorporation of UV-RA in the system. This was attributed to the combined effect of the crosslinking density, incorporation of phosphorus into the system, and the rigid benzene ring present in PPDC which increased the overall thermal stability of the coating formulations. Similar results were reflected in LOI and UL-94 tests as all the formulations could self-extinguish the fire, and 20UV-RA had the highest LOI value of 27. The mechanical properties did not vary much with the loading of UV-RA except for 20UV-RA which showed a slight decrement in the crosshatch adhesion, gloss, pencil hardness, and gel content values. As discussed in the flame-retardant properties of the coatings, one can try to develop an intermediate based on silicon using dichlorodimethylsilane (DCDMS) and can load it into the system for char enrichment as a future scope of this work.

References

1. Granzow, A, "Flame Retardation by Phosphorus Compunds." *Acc. Chem. Res.*, **5** (11) 177–183 (1978). https://doi.org/10.1177/0734904110395469
2. García, M, Hidalgo, J, Garmendia, I, "Composites: Part A Wood – Plastics Composites with Better Fire Retardancy and Durability Performance." *Compos Part A.*, **40** 1772–1776 (2009). https://doi.org/10.1016/j.compositesa.2009.08.010
3. Mark, H, "Flammability," *Encyclo. Polym. Sci. Tech. Con.*, Wiley (2013).
4. Chambhare, SU, Lokhande, GP, Jagtap, RN, "UV-Curable Behavior of Phosphorus- and Nitrogen-Based Reactive Diluent for Epoxy Acrylate Oligomer Used for Flame-Retardant Wood Coating." *J. Coat. Technol. Res.*, **13** (4) 703–714 (2016). https://doi.org/10.1007/s11998-015-9777-x
5. Nelson, G, Kinson, P, Quinn, C, "Fire Retardant Polymers." *Ann. Review Mater. Sci.*, **4** 391–414 (1974). https://doi.org/10.1146/annurev.ms.04.080174.002135
6. Bourbigot, S, Duquesne, S, "Fire Retardant Polymers: Recent Developments and Opportunities." *J. Mater. Chem.*, **17** 2283–2300 (2007). https://doi.org/10.1039/b702511d
7. Bourbigot, S, Flambard, X, "Heat Resistance and Flammability of High Performance Fibres: A Review." *Fire Mater.*, **168** 155–168 (2002). https://doi.org/10.1002/fam.799
8. Wang, Z, Han, E, Ke, W, "Influence of Nano-LDHs on Char Formation and Fire-Resistant Properties of Flame-Retar-

dant Coating.'' *Prog. Org. Coat.*, **53** (1) 29–37 (2005). https://doi.org/10.1016/j.porgcoat.2005.01.004
9. Pearce, E, Liepins, R, ''Flame Retardants.'' *Enviro. Health Persp.*, **11** 59–69 (1975)
10. Troitzsch, J, ''Overview of Flame Retardants,'' *Chem. Today.*, **16** (1998)
11. Chen, X, Hu, Y, Jiao, C, Song, L, ''Thermal and UV-Curing Behavior of Phosphate Diacrylate Used for Flame Retardant Coatings.'' *Prog. Org. Coat.*, **59** (4) 318–323 (2007)
12. Maiti, S, Banerjee, S, Palit, S, ''Phosphorus Containing Polymers.'' *Prog. Polym. Sci.*, **18** 227–261 (1993)
13. Huang, W, Chen, K, Yeh, J, Chen, K, ''Curing and Combustion Properties of a PU-Coating System with UV-Reactive Phosphazene.'' *J. App. Polym. Sci.*, **85** 1980–1991 (2002). https://doi.org/10.1002/app.10776
14. Patil, DM, Phalak, GA, Mhaske, ST, ''Design and Synthesis of Bio-Based UV Curable PU Acrylate Resin from Itaconic Acid for Coating Applications.'' *Des. Monomers Polym.*, **20** 269–282 (2017). https://doi.org/10.1080/15685551.2016.1231045
15. Lokhande, G, Chambhare, S, Jagtap, R, ''Synthesis and Properties of Phosphate-Based Diacrylate Reactive Diluent Applied to UV-Curable Flame-Retardant Wood Coating.'' *J. Coat. Technol. Res.*, **14** 255–266 (2017). https://doi.org/10.1007/s11998-016-9849-6
16. Shang, D, Sun, X, Hang, J, ''Flame Resistance, Physical and Mechanical Properties Of UV-Cured Hybrid Coatings Containing Low-Hydroxyl-Content Sols Via an Anhydrous Sol-Gel Process.'' *Prog. Org. Coat.*, **105** 267–276 (2017). https://doi.org/10.1016/j.porgcoat.2017.01.015
17. Wang, P, Yang, F, Li, L, Cai, Z, ''Flame Retardancy and Mechanical Properties of Epoxy Thermosets Modified with a Novel DOPO-Based Oligomer.'' *Polym. Degrad. Stab.*, **129** 156–167 (2016). https://doi.org/10.1016/j.polymdegradstab.2016.04.005
18. Sonnier, R, Dumazert, L, Livi, S, ''Flame Retardancy of Phosphorus-Containing Ionic Liquid Based Epoxy Networks.'' *Polym. Degrad. Stab.*, **134** 186–193 (2016). https://doi.org/10.1016/j.polymdegradstab.2016.10.009
19. Jeng, RJ, Shau, SM, Lin, JJ, ''Flame Retardant Epoxy Polymers Based on All Phosphorus-Containing Components.'' *Eur. Polym. J.*, **38** 683–693 (2012). https://doi.org/10.1016/S0014-3057(01)00246-4
20. Wang S, Xu C, Liu Y, et al., ''Vanillin-Derived High-Performance Flame Retardant Epoxy Resins: Facile Synthesis and Properties.'' (2017). https://doi.org/10.1021/acs.macromol.7b00097
21. Chen, X, Jiao, C, ''Thermal Degradation Characteristics of a Novel Flame Retardant Coating Using TG-IR Technique.'' *Polym Degrad Stab*, **93** 2222–2225 (2008). https://doi.org/10.1016/j.polymdegradstab.2008.09.005
22. Quin, L, Ye, L, Xu, G, Liu, J, *Polym Degrad Stab*, **96** 1118–1124 (2011)
23. Chuan, S, Ying, L, *Polymer (Guildf)*, **43** 4277–4284 (2002)
24. Choia, J, Seob, J, Khanc, S, *Prog. Org. Coat.*, **71** 110–116 (2011)
25. Liu Y, Hsiue G, Lan C, Chiu Y, 8-Flame-Retardant Polyurethanes from Phosphorus-Containing. 1769–1780 (1996)
26. Liu, YL, Hsiue, GH, Lan, CW, Chiu, YS, ''Phosphorus-Containing Epoxy for Flame Retardance: IV. Kinetics and Mechanism of Thermal Degradation.'' *Polym Degrad Stab*, **56** 291–299 (1997). https://doi.org/10.1016/S0141-3910(96)00177-2
27. Banerjee, S, Palit, SK, Maiti, S, ''Phosphorus Containing Polymers. 3. Polyimidophosphonates.'' *J Polym Sci Part A - Polym Chem*, **32** 219–227 (1994)
28. Castilla, E, Martín, N, Pardo, L, ''Minimum Phi-Divergence Estimators for Multinomial Logistic Regression with Complex Sample Design.'' *AStA Adv Stat Anal*, **102** 381–411 (2018). https://doi.org/10.1007/s10182-017-0311-6
29. Liu YL, Hsiue GH, Chiu YS, et al., ''Synthesis and Flame-retardant Properties of Phosphorus-containing Polymers Based on Poly(4-hydroxystyrene).'' *J Appl Polym Sci,* **59**:1619–1625 (1996). https://doi.org/10.1002/(SICI)1097-4628(19960307)59:10<1619::AID-APP14>3.0.CO;2-R
30. Liu Y, Hsiue G, Chiu Y, Properties of Phosphate-Based Epoxy Resins. Phosphate-based Epoxy Resins 565–574 (1996)
31. Chao, P, Li, Y, Gu, X, et al., ''Novel Phosphorus-Nitrogen-Silicon Flame Retardants and Their Application in Cycloaliphatic Epoxy Systems.'' *Polym Chem*, **6** 2977–2985 (2015). https://doi.org/10.1039/c4py01724b
32. Qian, X, Song, L, Bihe, Y, et al., ''Organic/Inorganic Flame Retardants Containing Phosphorus, Nitrogen and Silicon: Preparation and Their Performance on the Flame Retardancy of Epoxy Resins as a Novel Intumescent Flame Retardant System.'' *Mater Chem Phys*, **143** 1243–1252 (2014). https://doi.org/10.1016/j.matchemphys.2013.11.029